Appendix of "Integration of Preferences in Decomposition Multi-Objective Optimization"

Ke Li[1], Kalyanmoy Deb[2] and Xin Yao[3]

[1]College of Engineering, Mathematics and Physical Sciences, University of Exeter
[2]Department of Electrical and Computer Engineering, Michigan State University
[3]CERCIA, School of Computer Science, University of Birmingham
*Email: k.li@exeter.ac.uk, kdeb@egr.msu.edu, x.yao@cs.bham.ac.uk

1 Choosing Pivot Point

In NUMS, the pivot point $\mathbf{w}^p$ is used to represent the ROI on the simplex Ψ^m. In this paper, we use the projection of the DM supplied aspiration level vector $\mathbf{z}^r$ onto Ψ^m to serve this purpose. In theory, finding such projection is equivalent to solve the following minimization problem:

$$\mathbf{w}^p = \operatorname*{argmin}_{\mathbf{w}\in\Psi^m} \|\mathbf{w} - \mathbf{z}^r\| \tag{1}$$

As discussed in [1], the solution of (1) is nontrivial and there does not have an explicit form. Here, we use the theorem developed in [1] to find such projection. Algorithm 1 gives the corresponding pseudo-code and interested readers are recommended to [1] for detailed mathematical deductions.

Algorithm 1: Projection of $\mathbf{z}^r \in \mathbb{R}^m$ onto the simplex Ψ^m

Input: DM supplied aspiration level vector $\mathbf{z}^r$
Output: Pivot point $\mathbf{w}^p$ on Ψ^m

Sort $\mathbf{z}^r$ in ascending order as $z_1^r \leq \cdots \leq z_m^r$;
for $i \leftarrow m-1$ **to** 1 **do**
  $t_i \leftarrow \frac{\sum_{j=i+1}^{m} z_j^r - 1}{m-i}$;
  if $t_i \geq z_i^r$ **then**
    $\hat{t} \leftarrow t_i$;
    return $\mathbf{w}^p \leftarrow [\mathbf{z}^r - \hat{t}]_+$
$\hat{t} \leftarrow \frac{\sum_{j=1}^{m} z_j^r - 1}{m}$;
return $\mathbf{w}^p \leftarrow [\mathbf{z}^r - \hat{t}]_+$

2 Proof of Theorem 1

Proof. Let us use a specific example shown in Fig. 1 to prove this theorem. Suppose the reference points are originally generated by the Das and Dennis's method [2]. Therefore, reference points are distributed on an unit m-simplex. Let the centroid of this simplex, i.e., $\mathbf{w}^p = (\frac{1}{m}, \cdots, \frac{1}{m})^T$, be the

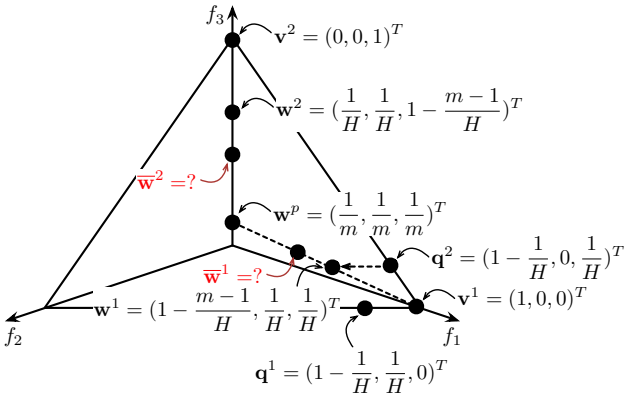

Figure 1: Illustrative example for η computation.

pivot point. Let us consider $\mathbf{v}^1 = (1,0,0)^T$ and $\mathbf{v}^2 = (0,0,1)^T$ as two vertices of an edge of this simplex. Obviously, the length of each edge of this simplex is the same, i.e., $\|\mathbf{v}^1 - \mathbf{v}^2\| = \sqrt{2}$. Suppose $\mathbf{w}^1$ and $\mathbf{w}^2$ are two reference points inside this simplex and closest to $\mathbf{v}^1$ and $\mathbf{v}^2$. Since reference points are generated in a structured manner, we can use a geometric method to find the coordinates of $\mathbf{w}^1$ and $\mathbf{w}^2$. As shown in Fig. 1, $\mathbf{q}^1$ and $\mathbf{q}^2$ are two reference points lying on the two edges and closest to $\mathbf{v}^1$. Obviously, $\mathbf{w}^1$ is a linear combination of $\mathbf{v}^1$, $\mathbf{q}^1$ and $\mathbf{q}^2$ as:

$$w_i^1 = (q_i^2 - v_i^1) + q_i^1 \tag{2}$$

where $i \in \{1, \cdots, m\}$. In summary, we can have $\mathbf{w}^1 = (1 - \frac{m-1}{H}, \cdots, \frac{1}{H})^T$ and $\mathbf{w}^2 = (\frac{1}{H}, \cdots, 1 - \frac{m-1}{H})^T$. Based on our non-uniform mapping scheme, we have the new locations of $\mathbf{w}^1$ and $\mathbf{w}^2$ can be calculated as:

$$\overline{\mathbf{w}}^i = \mathbf{w}^p + t \times \mathbf{u}^i \tag{3}$$

where $i \in \{1, 2\}$, $\mathbf{u}^i = \frac{\mathbf{v}^i - \mathbf{w}^p}{\|\mathbf{v}^i - \mathbf{w}^p\|}$ and

$$t = d - d(\frac{d - D}{d})^{\frac{1}{\eta+1}} \tag{4}$$

where $d = \|\mathbf{v^i} - \mathbf{w^p}\|$ and $D = \|\mathbf{w}^i - \mathbf{w}^p\|$. Let $q = \frac{d-D}{d}$, we have:

$$t = d(1 - q^{\frac{1}{\eta+1}}) \tag{5}$$

In order to have the extent of ROI become size of τ of the EF, we have the following equation:

$$\frac{\|\overline{\mathbf{w}}^1 - \overline{\mathbf{w}}^2\|}{\|\mathbf{v}^1 - \mathbf{v}^2\|} = \tau \tag{6}$$

Since $\|\mathbf{v}^1 - \mathbf{v}^2\| = \sqrt{2}$, we have:

$$\|\overline{\mathbf{w}}^1 - \overline{\mathbf{w}}^2\| = \sqrt{2}\tau \tag{7}$$

Using equation (3) to substitute $\overline{\mathbf{w}}^1$ and $\overline{\mathbf{w}}^2$ in equation (7), we have:

$$\|t \times (\mathbf{u}^1 - \mathbf{u}^2)\| = \sqrt{2}\tau \tag{8}$$

Using equation (5) to substitute t in equation (8), we have:

$$d(1 - q^{\frac{1}{\eta+1}}) \times \|\mathbf{u}^1 - \mathbf{u}^2\| = \sqrt{2}\tau \tag{9}$$

By substitution, we have:

$$\begin{aligned}(1-q^{\frac{1}{\eta+1}})\times\|\mathbf{v}^1-\mathbf{v}^2\| &= \sqrt{2}\tau \\ \Longrightarrow\ q^{\frac{1}{\eta+1}} &= 1-\tau \\ \Longrightarrow\ \eta &= \frac{\log q}{\log(1-\tau)}-1\end{aligned} \tag{10}$$

Since the coordinates of $\mathbf{v}^1$, $\mathbf{w}^1$ and $\mathbf{w}^p$ are known, we have:

$$\begin{aligned}d &= \sqrt{(1-\frac{1}{m})^2+(m-1)\frac{1}{m^2}} \\ &= \sqrt{1-\frac{1}{m}}\end{aligned} \tag{11}$$

and

$$\begin{aligned}D &= \sqrt{(1-\frac{m-1}{H}-\frac{1}{m})^2+(m-1)(\frac{1}{m}-\frac{1}{H})^2} \\ &= \sqrt{1-\frac{1}{m}}(1-\frac{m}{H}) \\ &= (1-\frac{m}{H})d\end{aligned} \tag{12}$$

Based on equation (11) and equation (12), we have:

$$\begin{aligned}q &= \frac{d-D}{d} \\ &= \frac{d-(1-\frac{m}{H})d}{d} \\ &= \frac{m}{H}\end{aligned} \tag{13}$$

■

3 Proof of Corollary 1

Proof. As discussed in Section III-D, we should set $\eta > 0$ in the NUMS. Thus, based on Theorem 1, we have:

$$\frac{\log\frac{m}{H}}{\log(1-\tau)} > 1 \tag{14}$$

Since $\frac{m}{H} < 1$ and $1-\tau < 1$, we have:

$$\log\frac{m}{H} \le \log(1-\tau) \implies 0 < \tau < 1-\frac{m}{H} \tag{15}$$

■

4 Proof of Corollary 2

Proof. The proof of this corollary is similar to the Theorem 1. Let us use Fig. 1 for illustration again. As for the reference points $\mathbf{w}^1$ and $\mathbf{w}^2$, we should have the following relationship after the

non-uniform mapping:

$$\frac{\|\overline{\mathbf{w}}^1 - \overline{\mathbf{w}}^2\|}{\|\mathbf{w}^1 - \mathbf{w}^2\|} = \tau \tag{16}$$

Since $\|\mathbf{w}^1 - \mathbf{w}^2\| = \sqrt{2}(1 - \frac{m}{H})$, we have:

$$\|\overline{\mathbf{w}}^1 - \overline{\mathbf{w}}^2\| = \sqrt{2}(1 - \frac{m}{H})\tau \tag{17}$$

Using equation (3) to substitute $\overline{\mathbf{w}}^1$ and $\overline{\mathbf{w}}^2$ in equation (17), we have:

$$\|t \times (\mathbf{u}^1 - \mathbf{u}^2)\| = \sqrt{2}(1 - \frac{m}{H})\tau \tag{18}$$

Using equation (5) to substitute t in equation (18), we have:

$$d(1 - q^{\frac{1}{\eta+1}}) \times \|\mathbf{u}^1 - \mathbf{u}^2\| = \sqrt{2}(1 - \frac{m}{H})\tau \tag{19}$$

Since $\|\mathbf{v}^1 - \mathbf{v}^2\| = \sqrt{2}$, by substitution, we have:

$$\begin{aligned} 1 - q^{\frac{1}{\eta+1}} &= (1 - \frac{m}{H})\tau \\ \implies \eta &= \frac{\log q}{\log[1 - (1 - \frac{m}{H})\tau]} - 1 \end{aligned} \tag{20}$$

where $q = \frac{m}{H}$ according to equation (13). ■

5 Proof of Corollary 3

Proof. Since $\eta > 0$, according to equation (20), we have:

$$\frac{\log q}{\log[1 - (1 - \frac{m}{H})\tau]} > 1 \tag{21}$$

Since $\frac{m}{H} < 1$ and $1 - (1 - \frac{m}{H})\tau < 1$, we have:

$$\log \frac{m}{H} < \log\left[1 - (1 - \frac{m}{H})\tau\right] \implies 0 < \tau < 1 \tag{22}$$

■

6 Plots of Final Populations

This section provides the visual comparisons of different preference-based EMO algorithms. In particular, we plot the final solutions obtained by different algorithms that achieve the best R-IGD value.

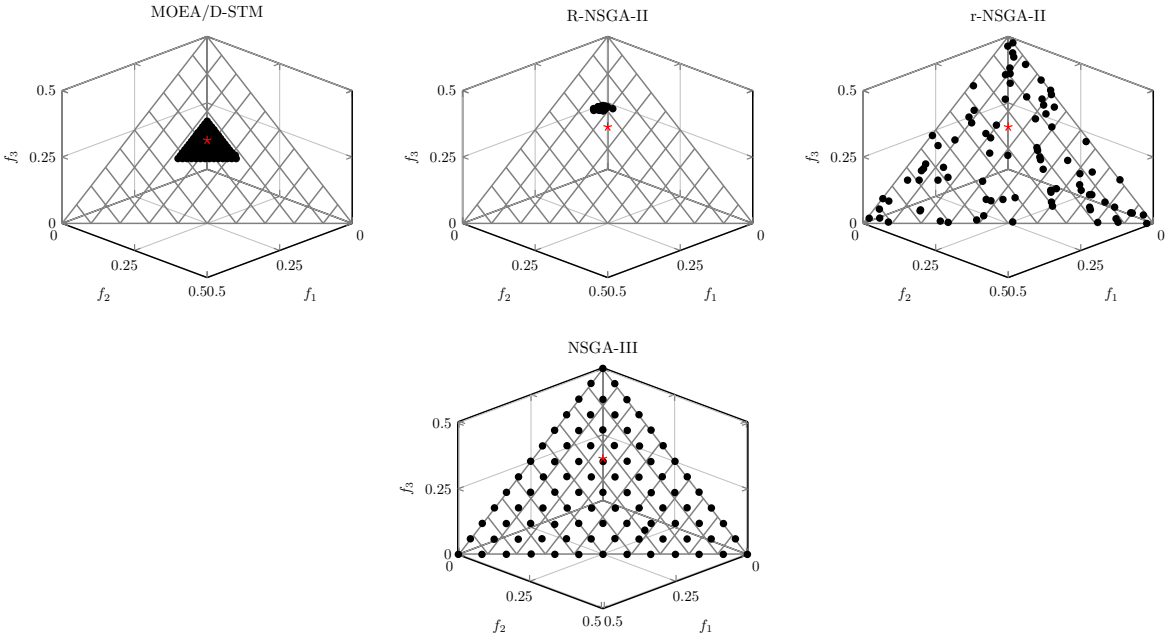

Figure 2: Comparisons on 3-objective DTLZ1 where $\mathbf{z}^r = (0.05, 0.05, 0.2)$.

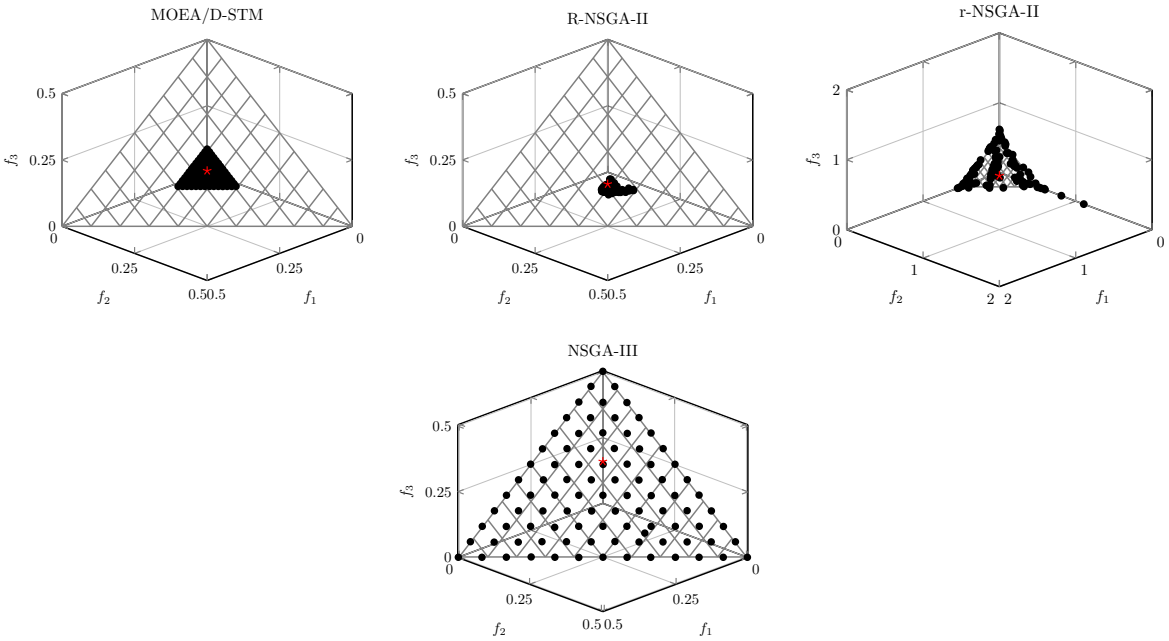

Figure 3: Comparisons on 3-objective DTLZ1 where $\mathbf{z}^r = (0.3, 0.3, 0.2)$.

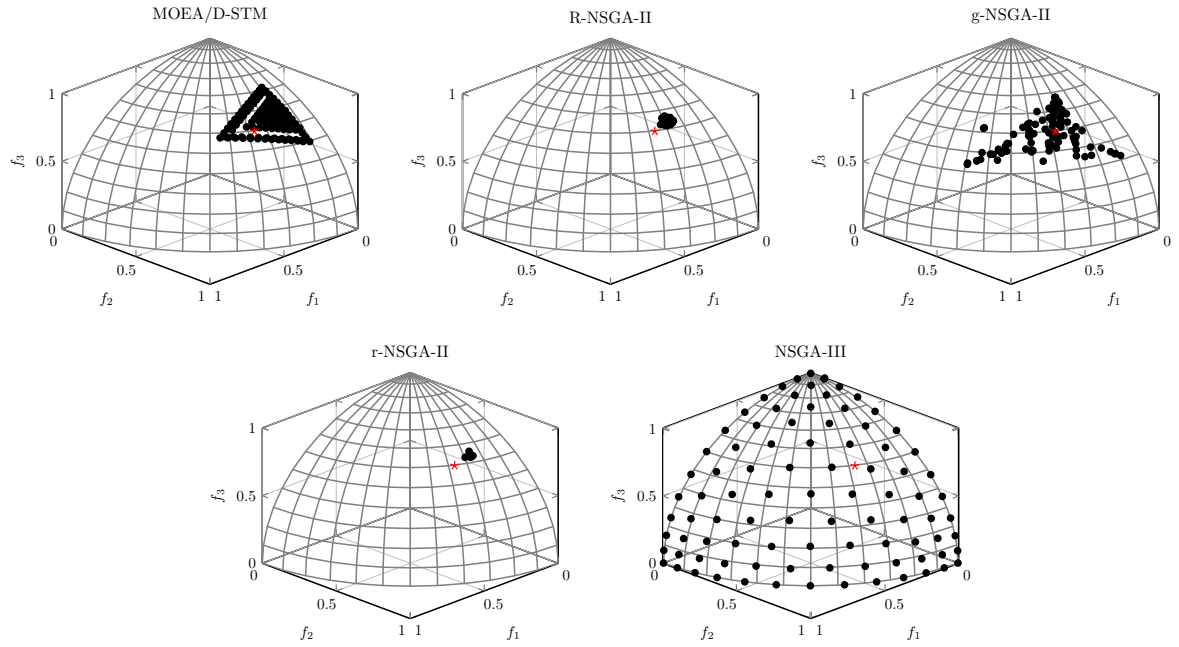

Figure 4: Comparisons on 3-objective DTLZ2 where $\mathbf{z}^r = (0.2, 0.5, 0.6)$.

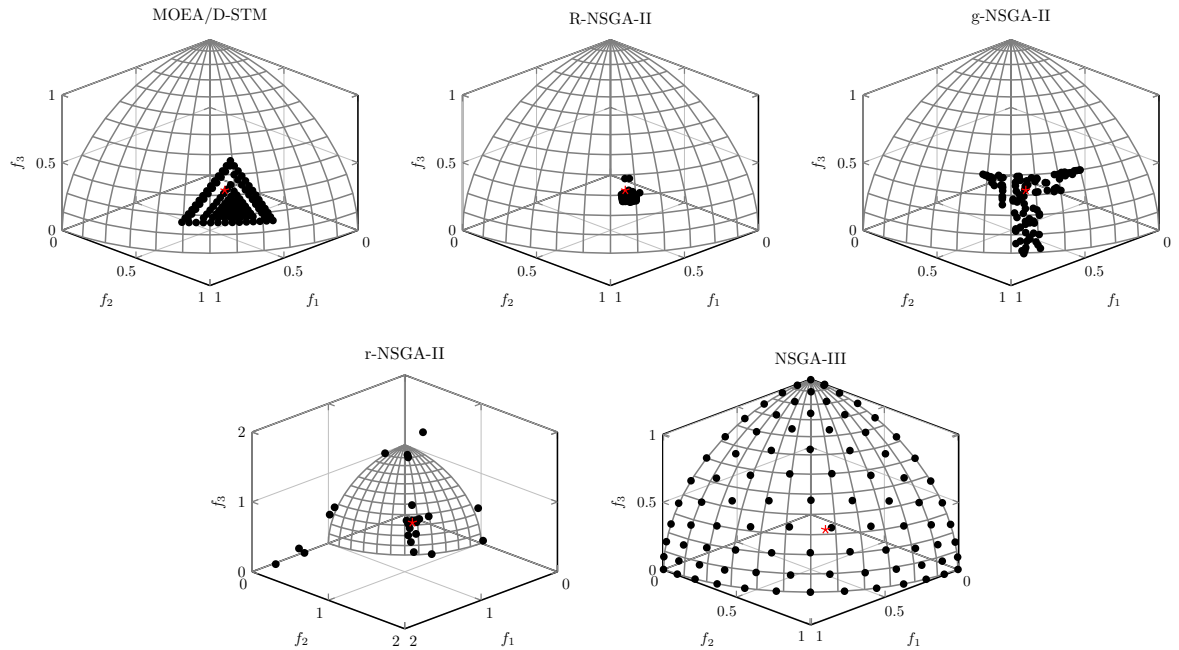

Figure 5: Comparisons on 3-objective DTLZ2 where $\mathbf{z}^r = (0.7, 0.8, 0.5)$.

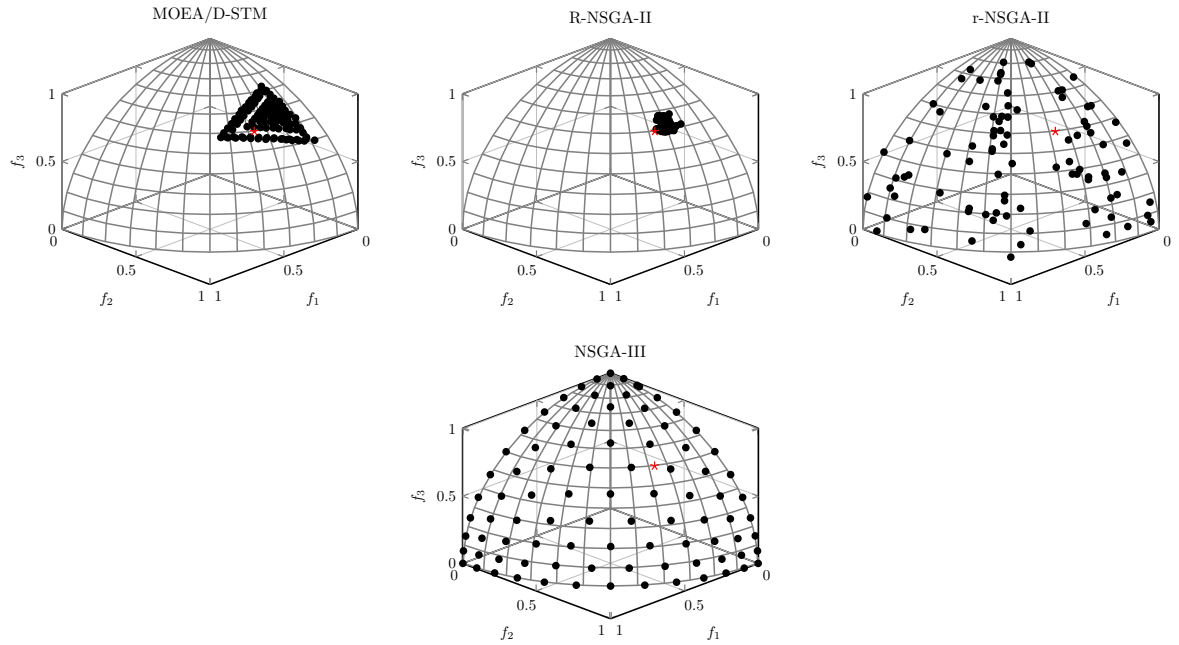

Figure 6: Comparisons on 3-objective DTLZ3 where $\mathbf{z}^r = (0.2, 0.5, 0.6)$.

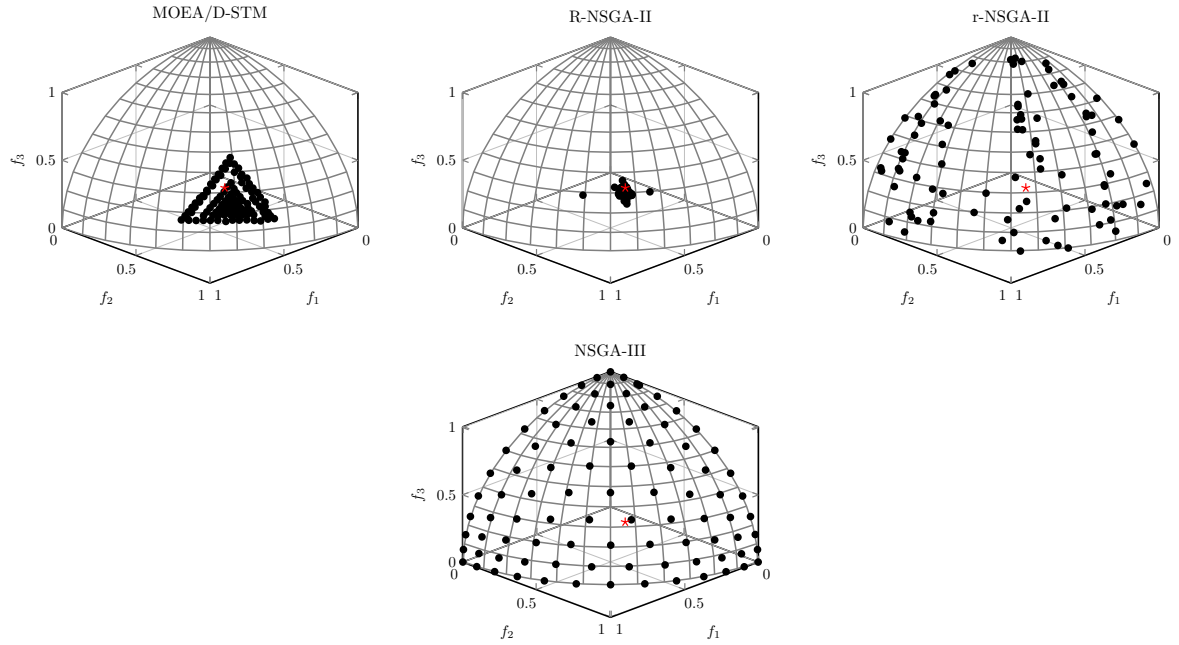

Figure 7: Comparisons on 3-objective DTLZ3 where $\mathbf{z}^r = (0.7, 0.8, 0.5)$.

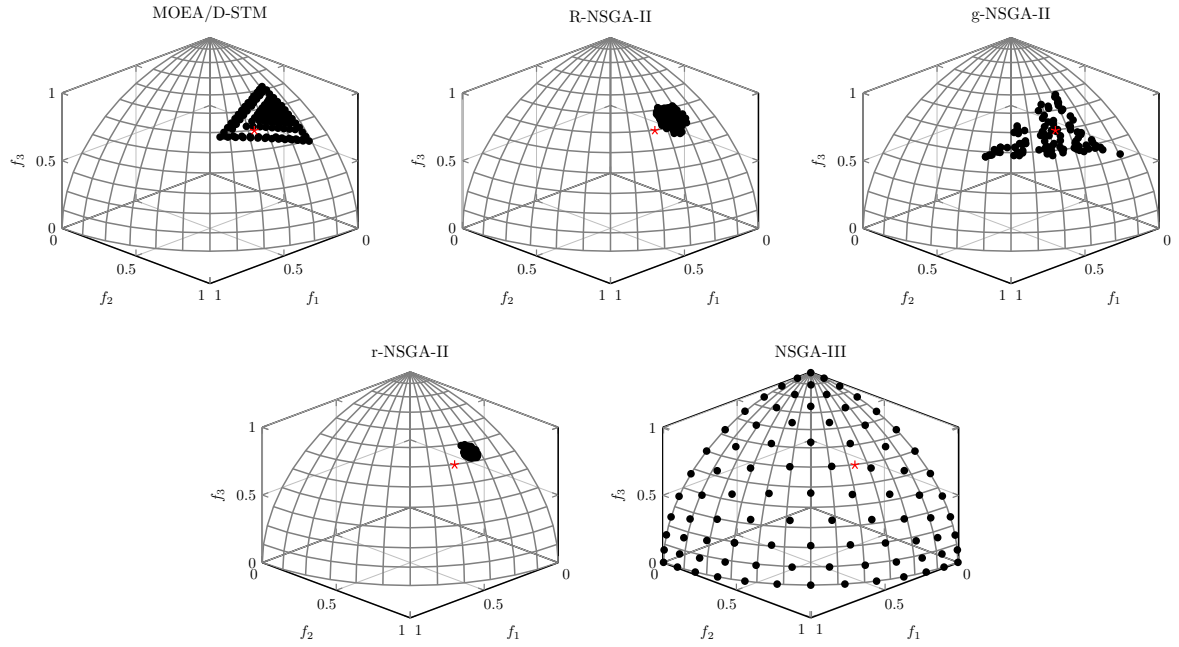

Figure 8: Comparisons on 3-objective DTLZ4 where $\mathbf{z}^r = (0.2, 0.5, 0.6)$.

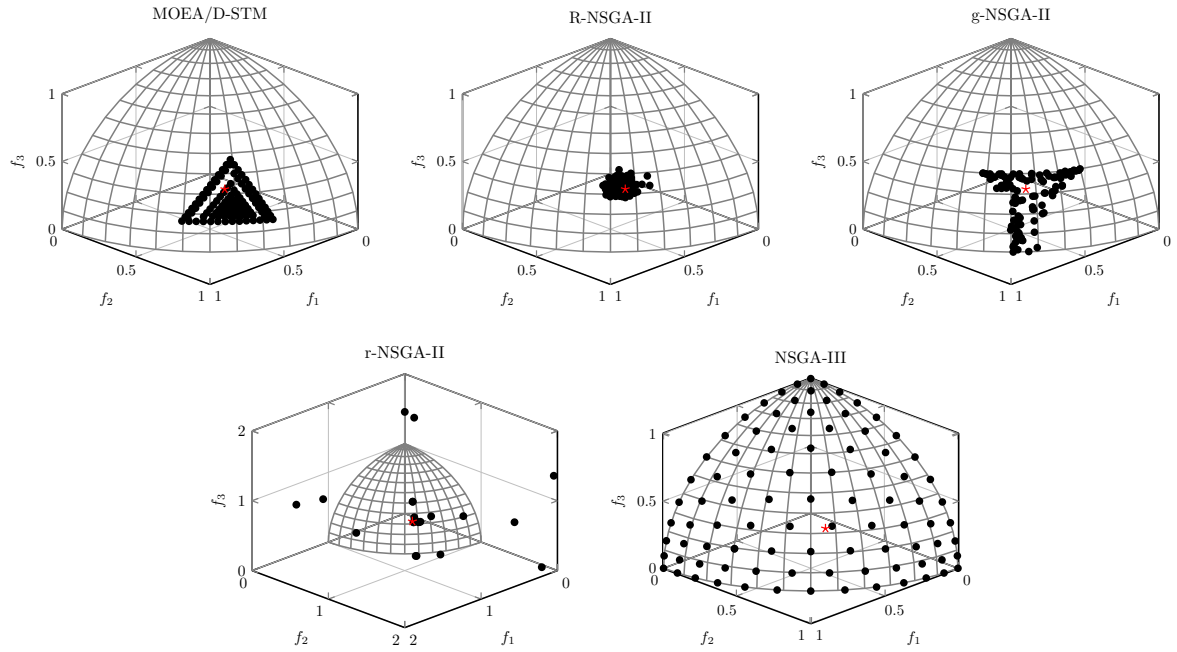

Figure 9: Comparisons on 3-objective DTLZ4 where $\mathbf{z}^r = (0.7, 0.8, 0.5)$.

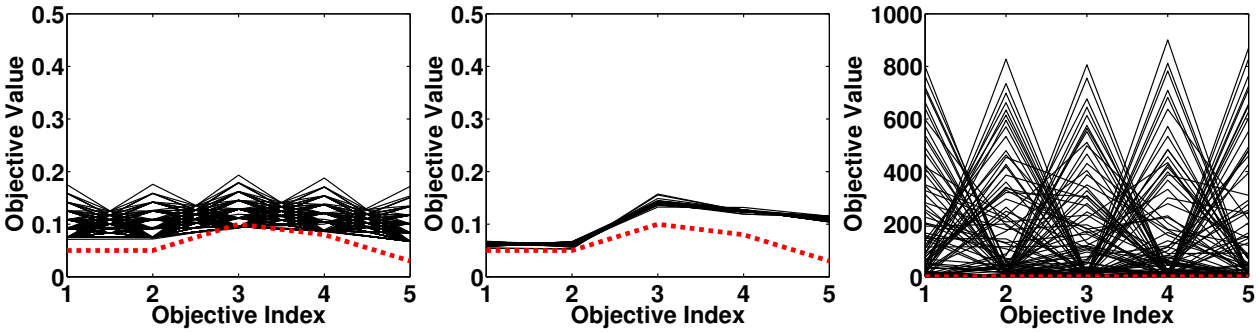

(a) MOEA/D-STM (b) R-NSGA-II (c) g-NSGA-II

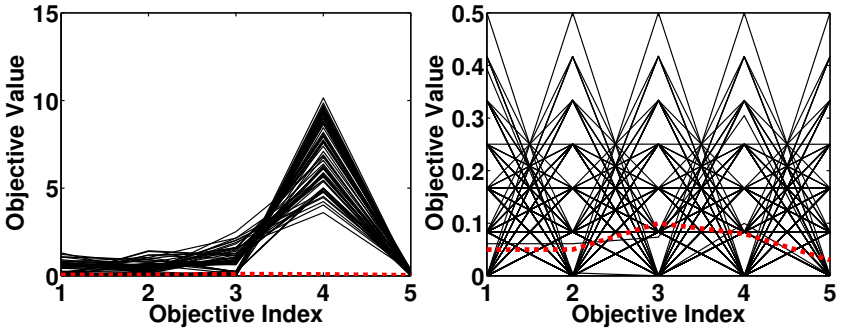

(d) r-NSGA-II (e) NSGA-III

Figure 10: Comparisons on 5-objective DTLZ1 where $\mathbf{z}^r = (0.05, 0.05, 0.1, 0.08, 0.03)^T$.

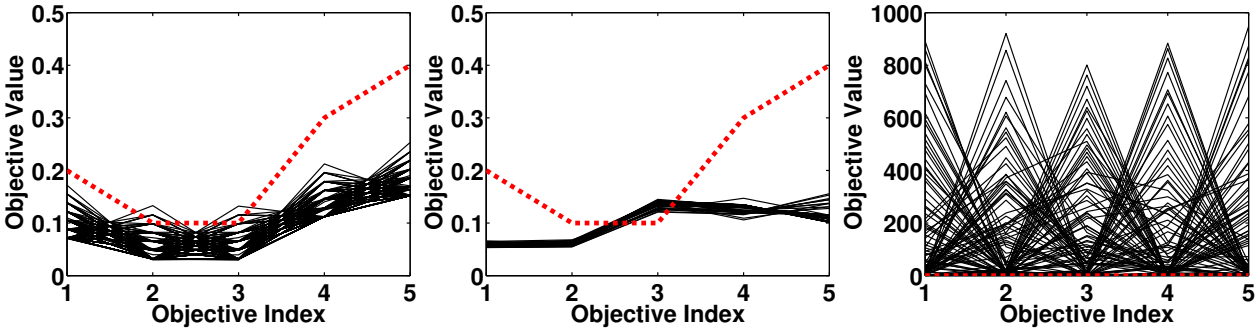

(a) MOEA/D-STM (b) R-NSGA-II (c) g-NSGA-II

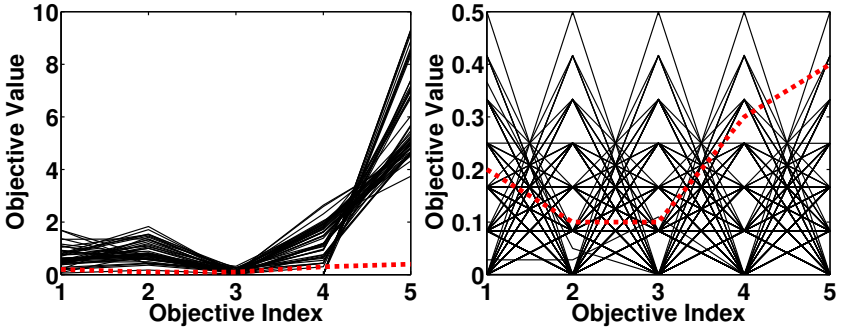

(d) r-NSGA-II (e) NSGA-III

Figure 11: Comparisons on 5-objective DTLZ1 where $\mathbf{z}^r = (0.2, 0.1, 0.1, 0.3, 0.4)^T$.

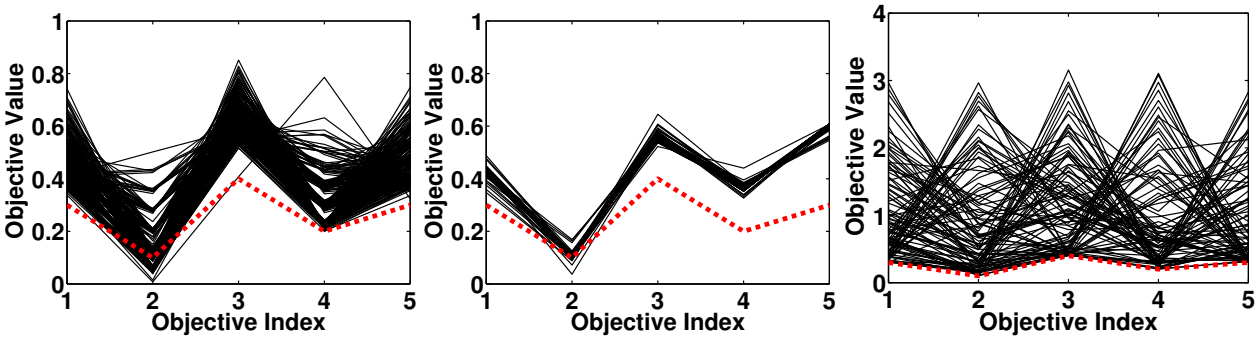

(a) MOEA/D-STM (b) R-NSGA-II (c) g-NSGA-II

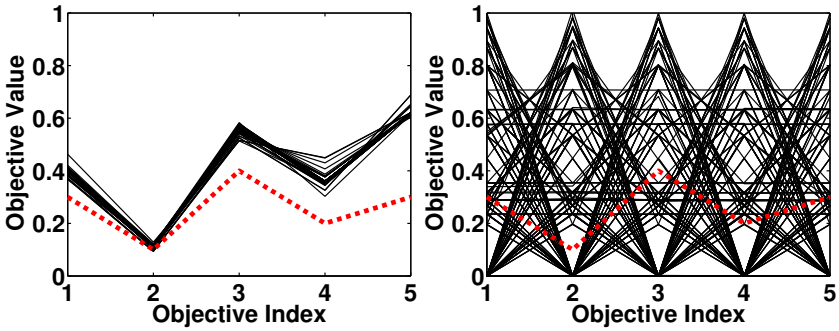

(d) r-NSGA-II (e) NSGA-III

Figure 12: Comparisons on 5-objective DTLZ2 where $\mathbf{z}^r = (0.3, 0.1, 0.4, 0.2, 0.3)^T$.

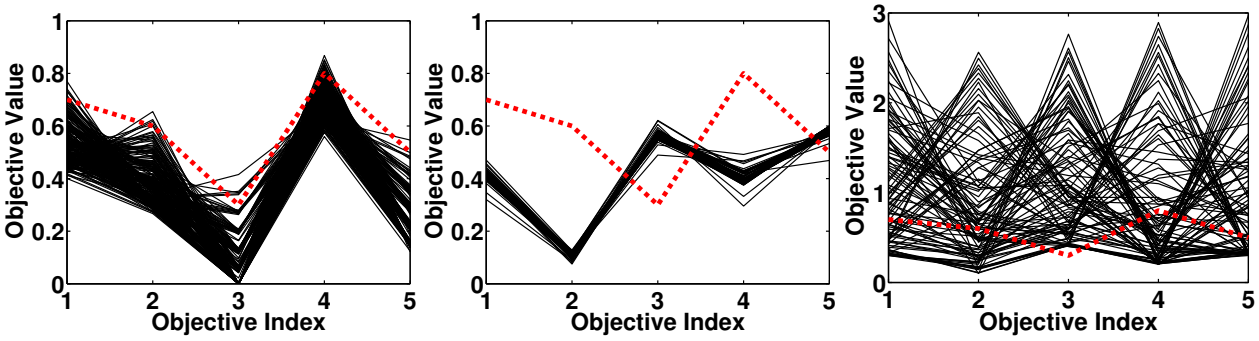

(a) MOEA/D-STM (b) R-NSGA-II (c) g-NSGA-II

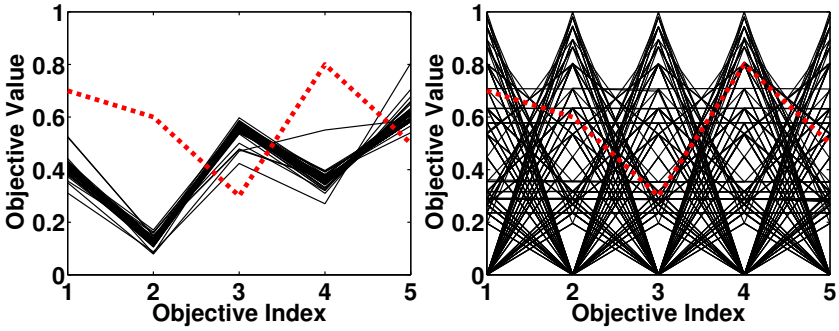

(d) r-NSGA-II (e) NSGA-III

Figure 13: Comparisons on 5-objective DTLZ2 where $\mathbf{z}^r = (0.7, 0.6, 0.3, 0.8, 0.5)^T$.

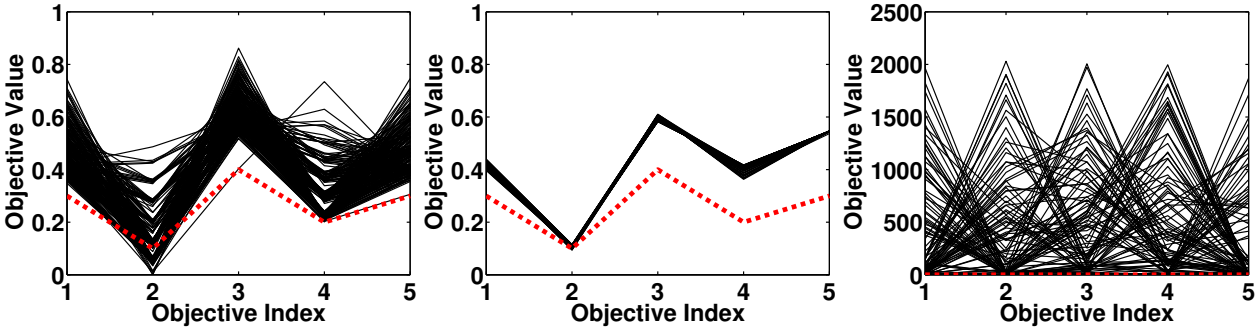

(a) MOEA/D-STM (b) R-NSGA-II (c) g-NSGA-II

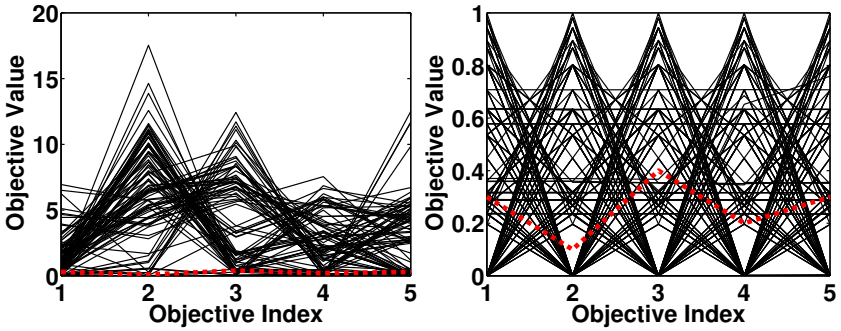

(d) r-NSGA-II (e) NSGA-III

Figure 14: Comparisons on 5-objective DTLZ3 where $\mathbf{z}^r = (0.3, 0.1, 0.4, 0.2, 0.3)^T$.

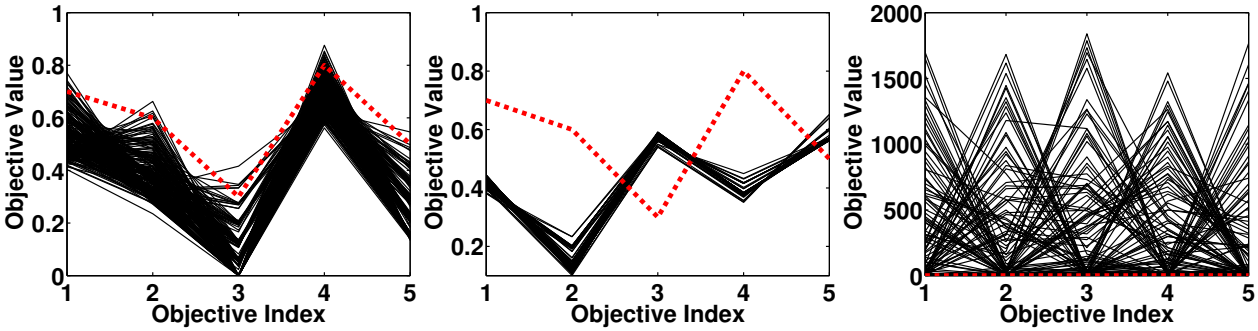

(a) MOEA/D-STM (b) R-NSGA-II (c) g-NSGA-II

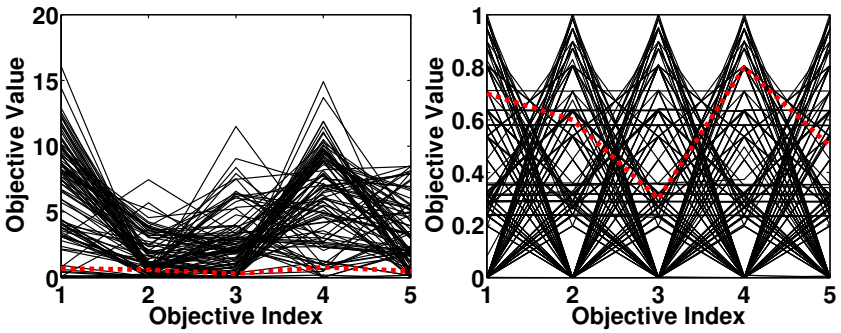

(d) r-NSGA-II (e) NSGA-III

Figure 15: Comparisons on 5-objective DTLZ3 where $\mathbf{z}^r = (0.7, 0.6, 0.3, 0.8, 0.5)^T$.

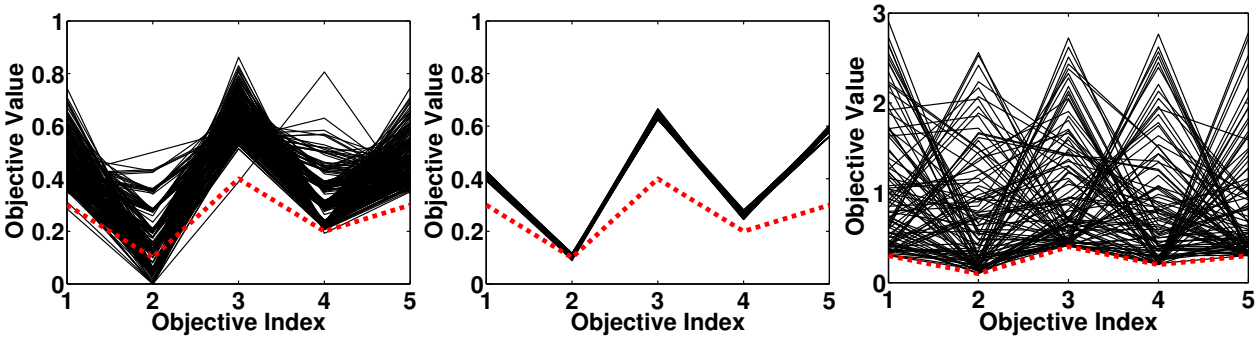

(a) MOEA/D-STM (b) R-NSGA-II (c) g-NSGA-II

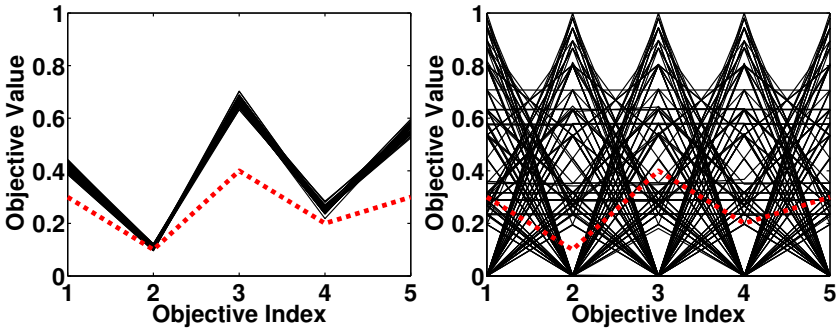

(d) r-NSGA-II (e) NSGA-III

Figure 16: Comparisons on 5-objective DTLZ4 where $\mathbf{z}^r = (0.3, 0.1, 0.4, 0.2, 0.3)^T$.

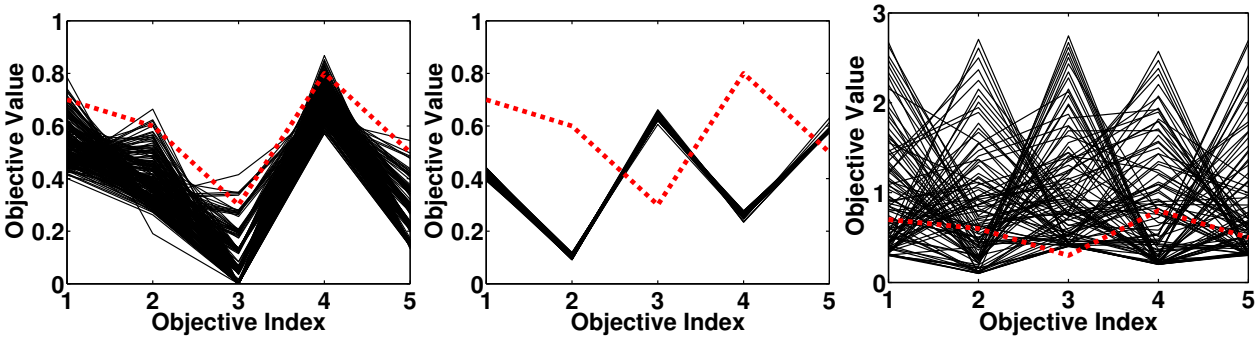

(a) MOEA/D-STM (b) R-NSGA-II (c) g-NSGA-II

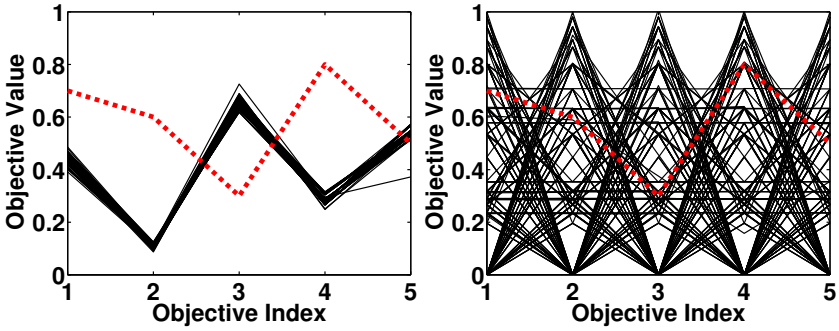

(d) r-NSGA-II (e) NSGA-III

Figure 17: Comparisons on 5-objective DTLZ4 where $\mathbf{z}^r = (0.7, 0.6, 0.3, 0.8, 0.5)^T$.

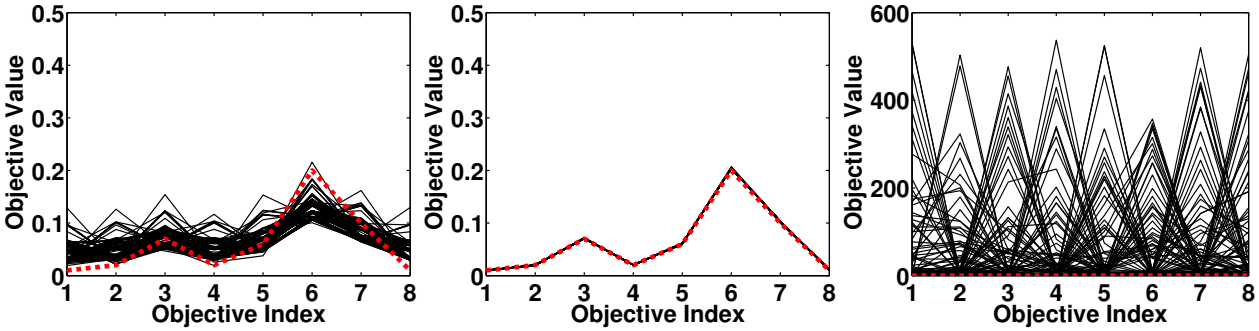

(a) MOEA/D-STM (b) R-NSGA-II (c) g-NSGA-II

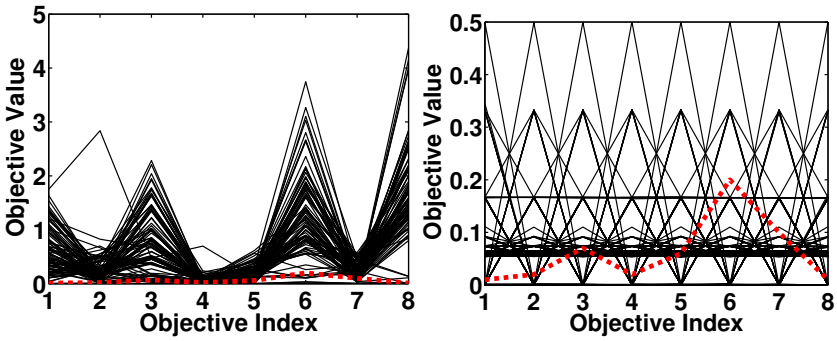

(d) r-NSGA-II (e) NSGA-III

Figure 18: Comparisons on 8-objective DTLZ1 where $\mathbf{z}^r = (0.01, 0.02, 0.07, 0.02, 0.06, 0.2, 0.1, 0.01)^T$.

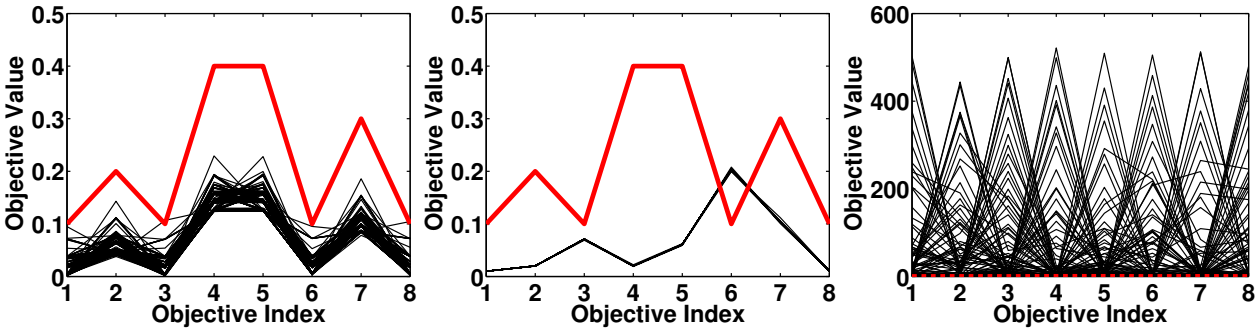

(a) MOEA/D-STM (b) R-NSGA-II (c) g-NSGA-II

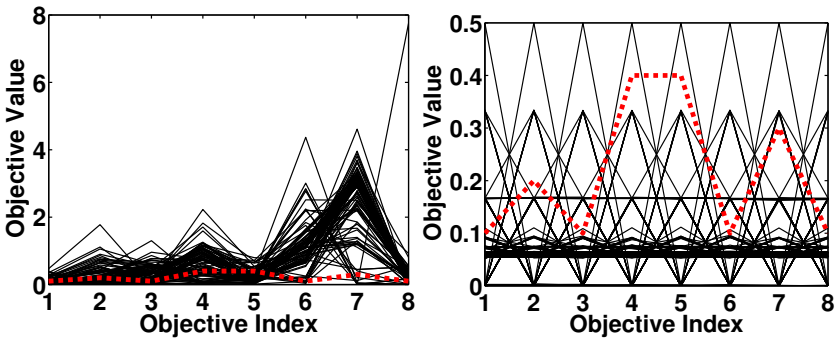

(d) r-NSGA-II (e) NSGA-III

Figure 19: Comparisons on 8-objective DTLZ1 where $\mathbf{z}^r = (0.1, 0.2, 0.1, 0.4, 0.4, 0.1, 0.3, 0.1)^T$.

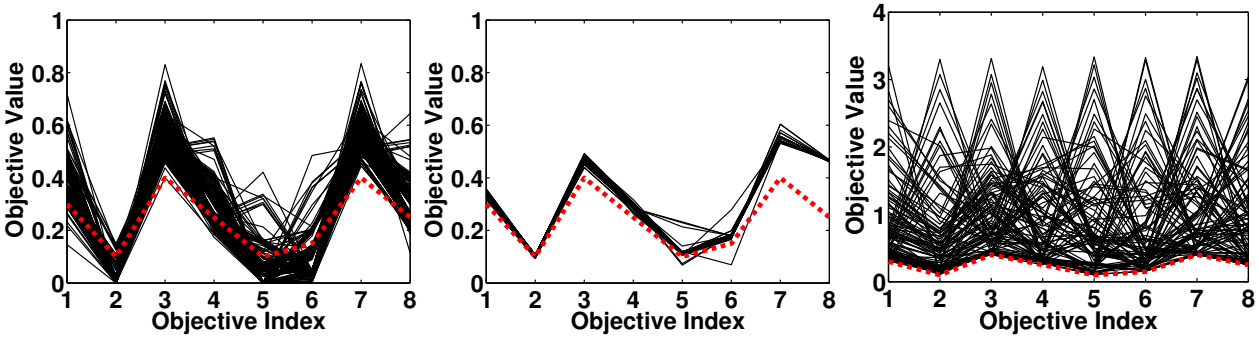

(a) MOEA/D-STM (b) R-NSGA-II (c) g-NSGA-II

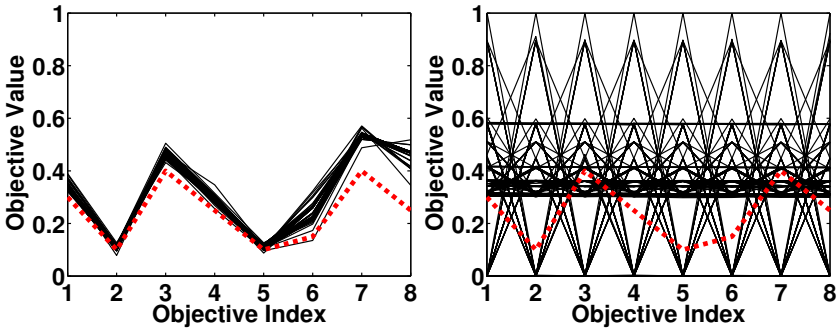

(d) r-NSGA-II (e) NSGA-III

Figure 20: Comparisons on 8-objective DTLZ2 where $\mathbf{z}^r = (0.3, 0.1, 0.4, 0.25, 0.1, 0.15, 0.4, 0.25)^T$.

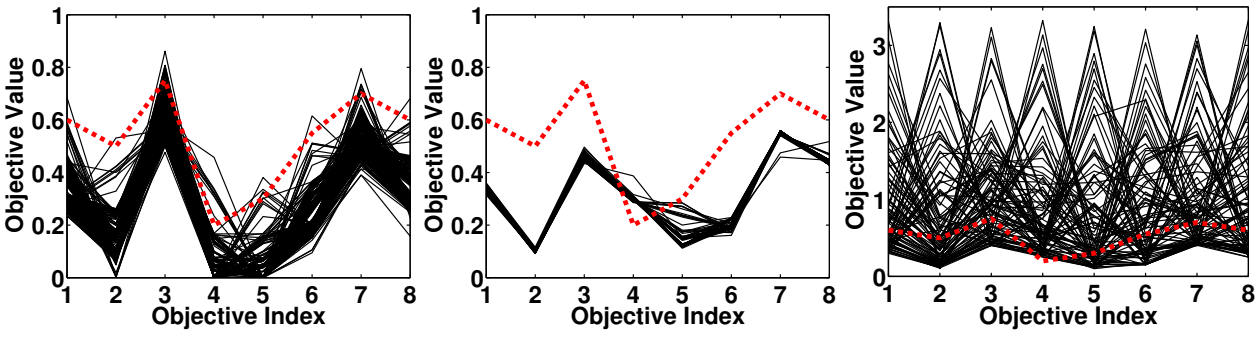

(a) MOEA/D-STM (b) R-NSGA-II (c) g-NSGA-II

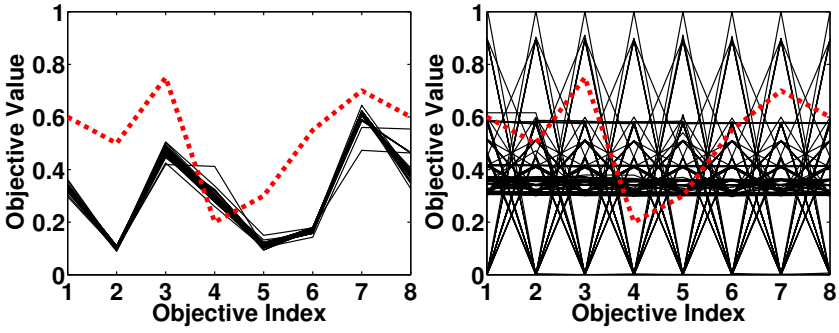

(d) r-NSGA-II (e) NSGA-III

Figure 21: Comparisons on 8-objective DTLZ2 where $\mathbf{z}^r = (0.6, 0.5, 0.75, 0.2, 0.3, 0.55, 0.7, 0.6)^T$.

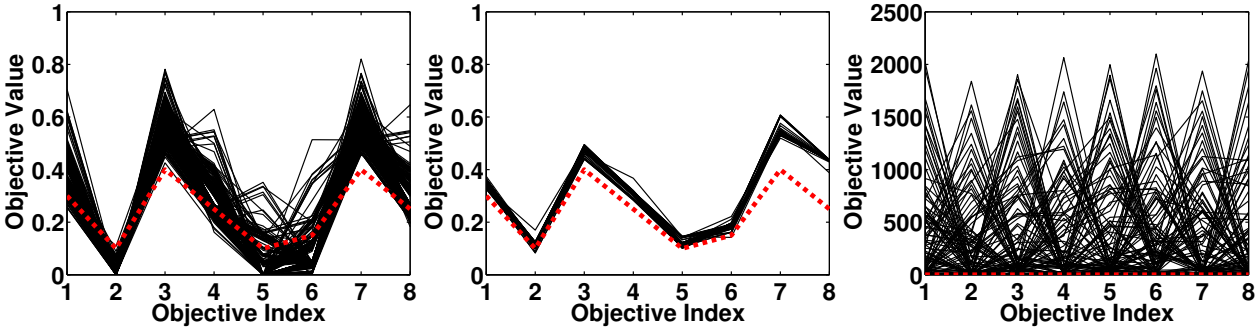

(a) MOEA/D-STM (b) R-NSGA-II (c) g-NSGA-II

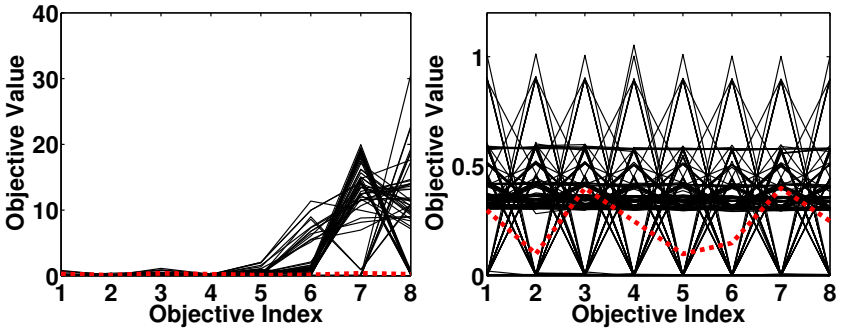

(d) r-NSGA-II (e) NSGA-III

Figure 22: Comparisons on 8-objective DTLZ3 where $\mathbf{z}^r = (0.3, 0.1, 0.4, 0.25, 0.1, 0.15, 0.4, 0.25)^T$.

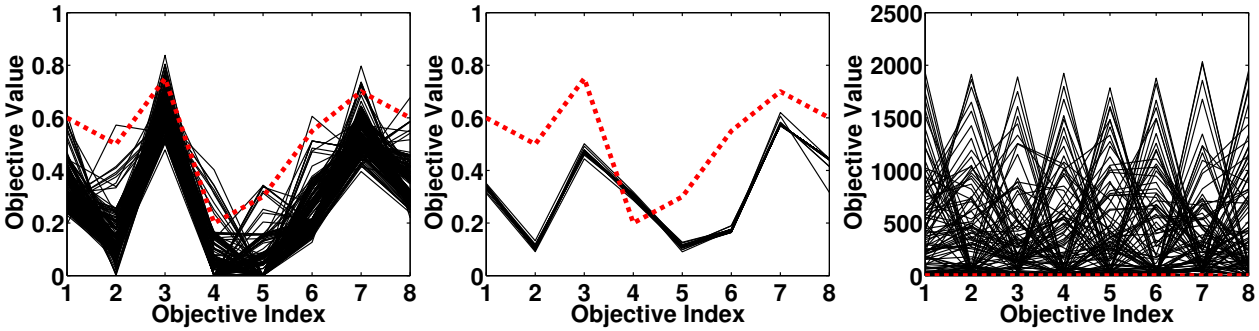

(a) MOEA/D-STM (b) R-NSGA-II (c) g-NSGA-II

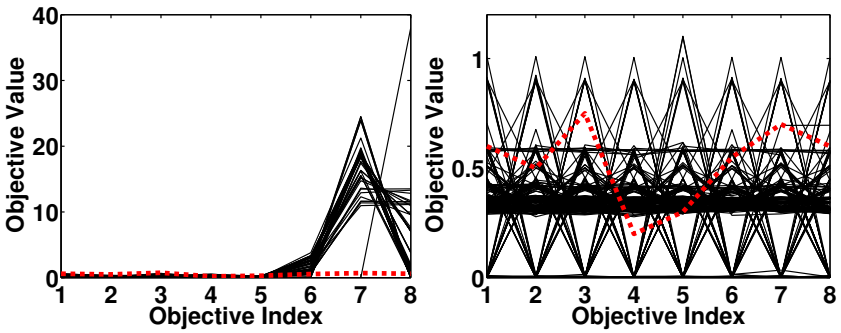

(d) r-NSGA-II (e) NSGA-III

Figure 23: Comparisons on 8-objective DTLZ3 where $\mathbf{z}^r = (0.6, 0.5, 0.75, 0.2, 0.3, 0.55, 0.7, 0.6)^T$.

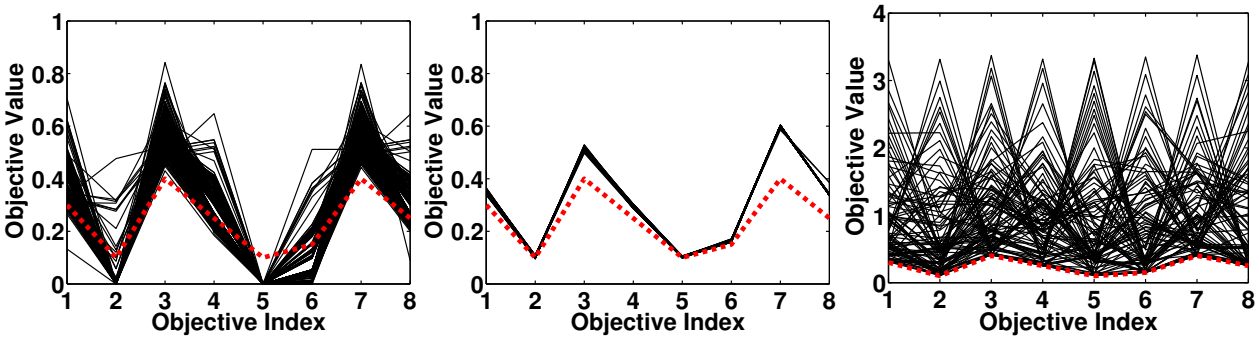

(a) MOEA/D-STM (b) R-NSGA-II (c) g-NSGA-II

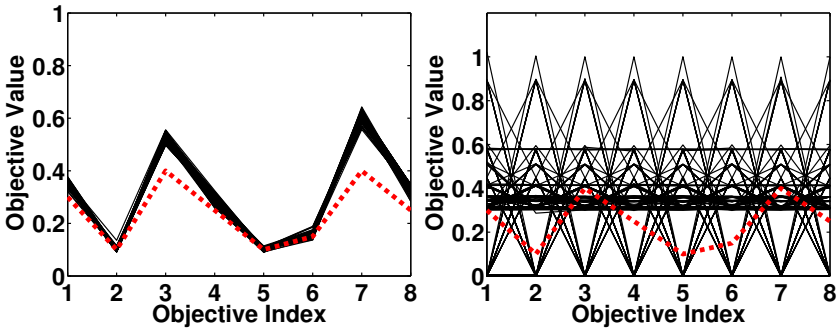

(d) r-NSGA-II (e) NSGA-III

Figure 24: Comparisons on 8-objective DTLZ4 where $\mathbf{z}^r = (0.3, 0.1, 0.4, 0.25, 0.1, 0.15, 0.4, 0.25)^T$.

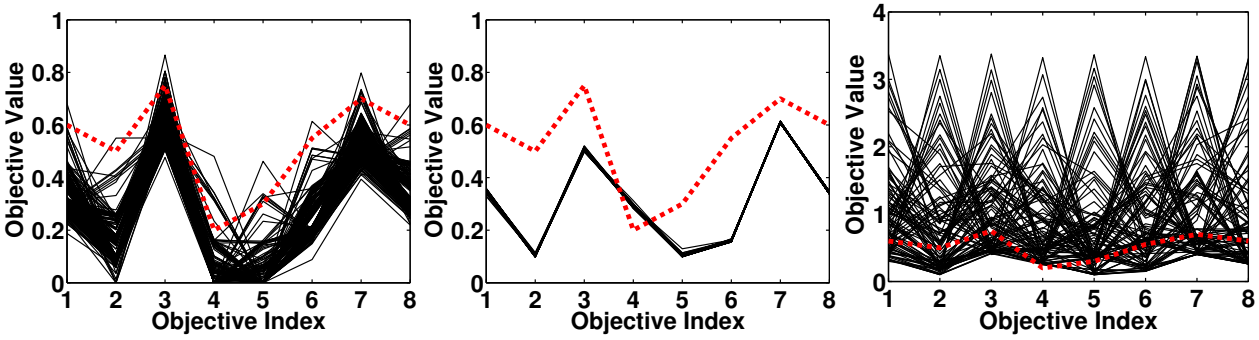

(a) MOEA/D-STM (b) R-NSGA-II (c) g-NSGA-II

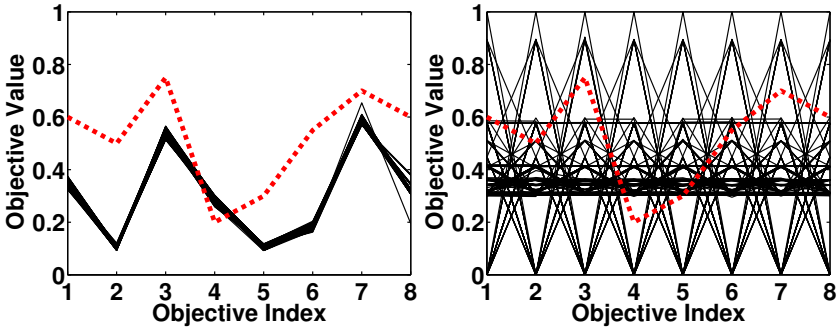

(d) r-NSGA-II (e) NSGA-III

Figure 25: Comparisons on 8-objective DTLZ4 where $\mathbf{z}^r = (0.6, 0.5, 0.75, 0.2, 0.3, 0.55, 0.7, 0.6)^T$.

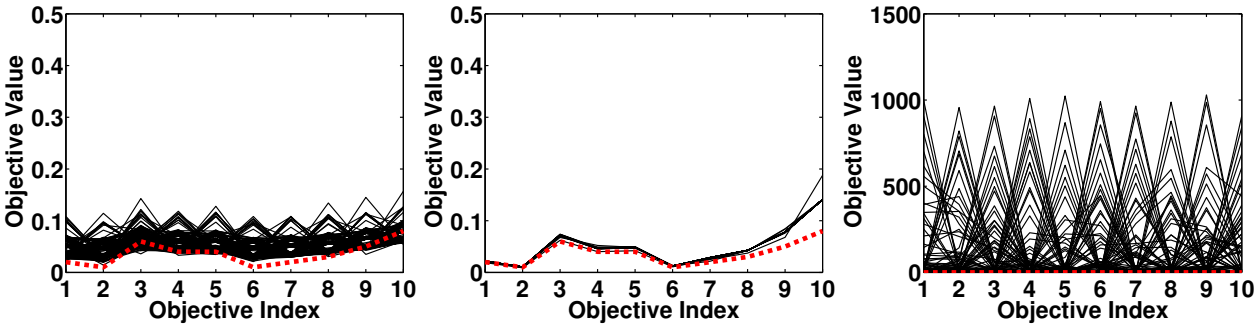

(a) MOEA/D-STM (b) R-NSGA-II (c) g-NSGA-II

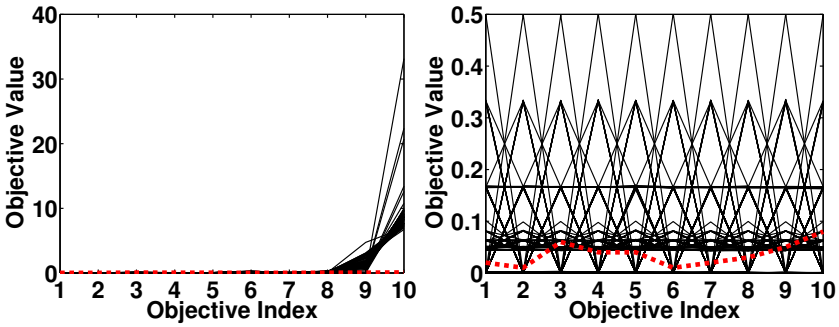

(d) r-NSGA-II (e) NSGA-III

Figure 26: Comparisons on 10-objective DTLZ1 where $\mathbf{z}^r = (0.02, 0.01, 0.06, 0.04, 0.04, 0.01, 0.02, 0.03, 0.05, 0.08)^T$.

References

[1] Y. Chen and X. Ye, "Projection onto a simplex," *ArXiv e-prints*, Jan 2011.

[2] I. Das and J. E. Dennis, "Normal-Boundary Intersection: A new method for generating the pareto surface in nonlinear multicriteria optimization problems," *SIAM Journal on Optimization*, vol. 8, pp. 631–657, 1998.

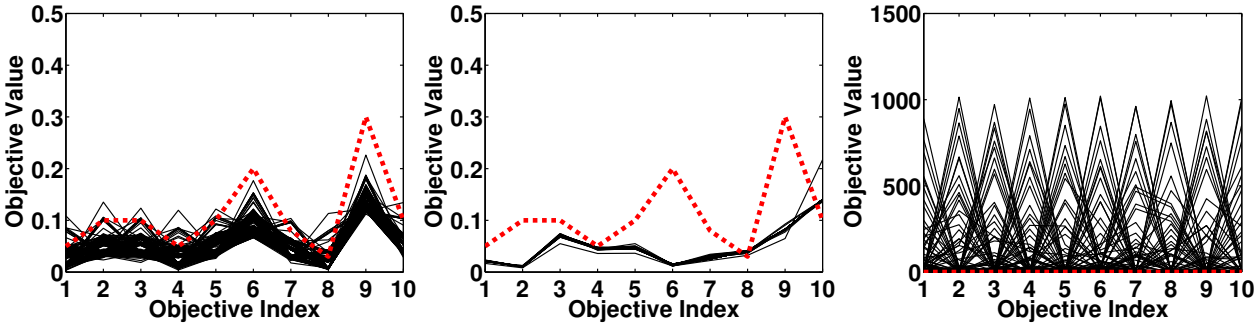

(a) MOEA/D-STM (b) R-NSGA-II (c) g-NSGA-II

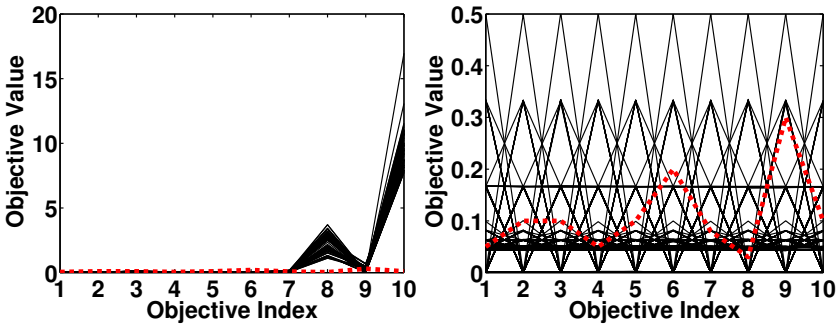

(d) r-NSGA-II (e) NSGA-III

Figure 27: Comparisons on 10-objective DTLZ1 where $\mathbf{z}^r = (0.05, 0.1, 0.1, 0.05, 0.1, 0.2, 0.08, 0.03, 0.3, 0.1)^T$.

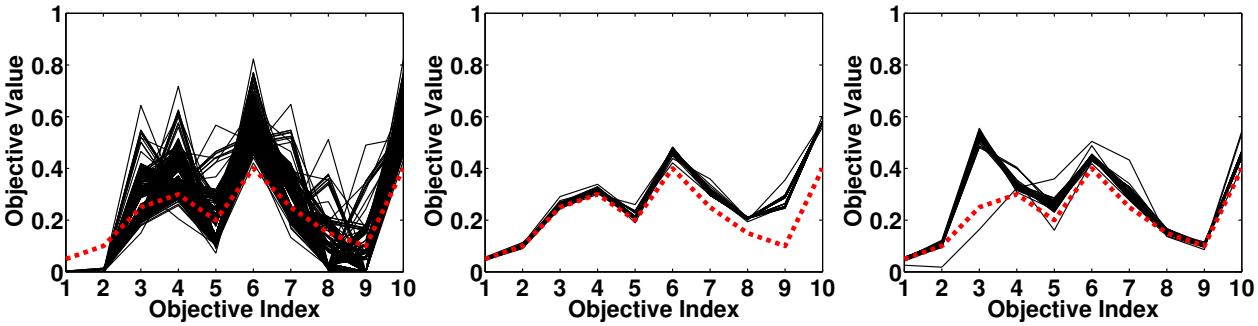

(a) MOEA/D-STM (b) R-NSGA-II (c) r-NSGA-II

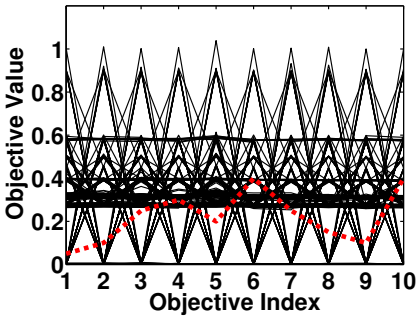

(d) NSGA-III

Figure 28: Comparisons on 10-objective DTLZ2 where $\mathbf{z}^r = (0.05, 0.1, 0.25, 0.3, 0.2, 0.4, 0.25, 0.15, 0.1, 0.4)^T$.

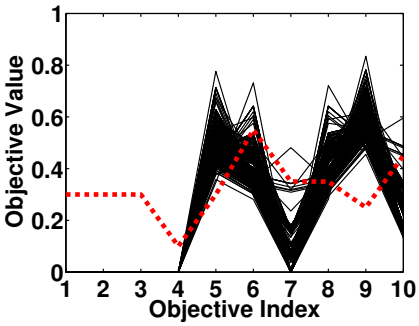

(a) MOEA/D-STM

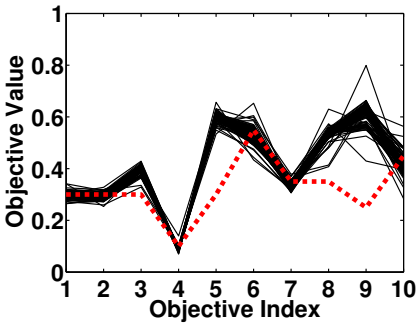

(b) R-NSGA-II

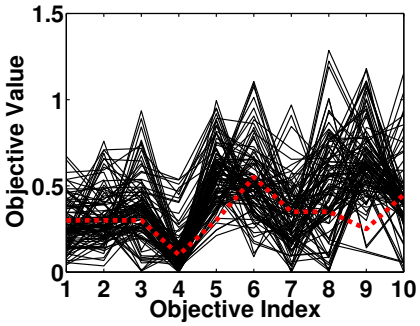

(c) NSGA-III

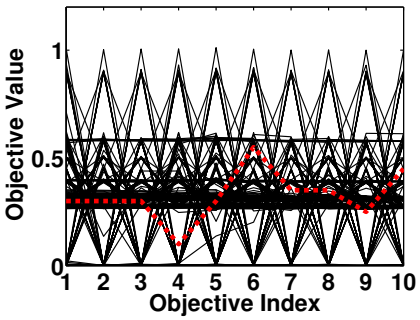

(d) NSGA-III

Figure 29: Comparisons on 10-objective DTLZ2 where $\mathbf{z}^r = (0.3, 0.3, 0.3, 0.1, 0.3, 0.55, 0.35, 0.35, 0.25, 0.45)^T$.

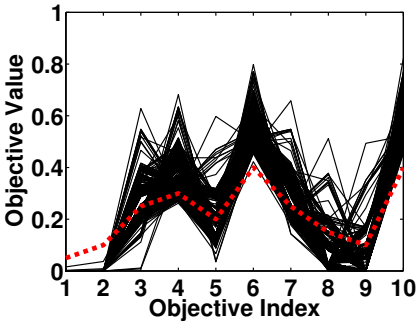

(a) MOEA/D-STM

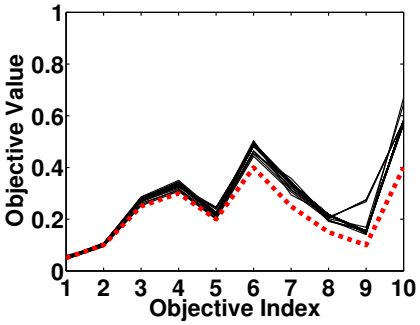

(b) R-NSGA-II

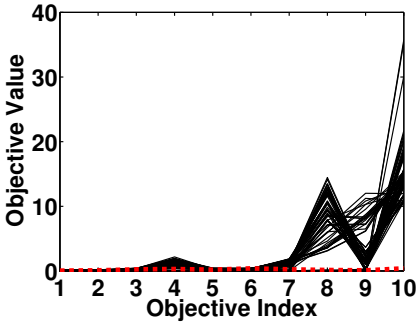

(c) r-NSGA-II

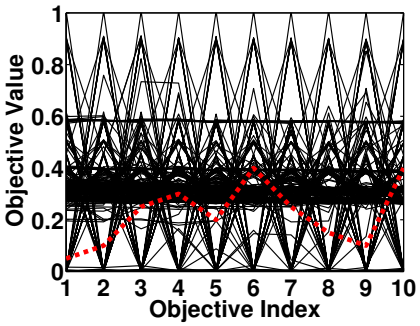

(d) NSGA-III

Figure 30: Comparisons on 10-objective DTLZ3 where $\mathbf{z}^r = (0.05, 0.1, 0.25, 0.3, 0.2, 0.4, 0.25, 0.15, 0.1, 0.4)^T$.

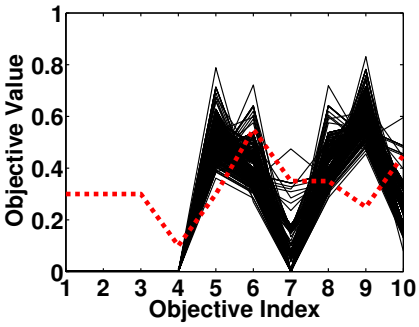

(a) MOEA/D-STM

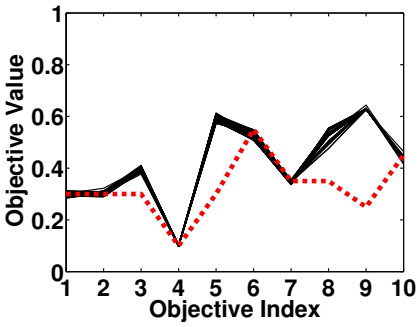

(b) R-NSGA-II

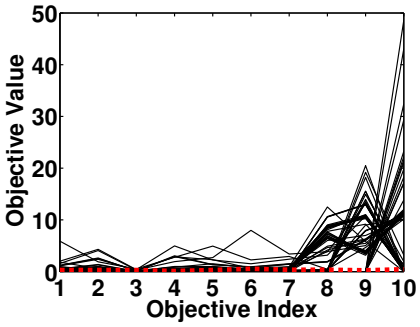

(c) r-NSGA-II

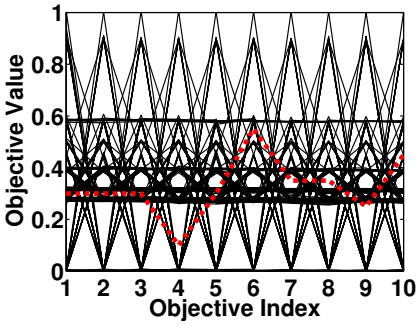

(d) NSGA-III

Figure 31: Comparisons on 10-objective DTLZ3 where $\mathbf{z}^r = (0.3, 0.3, 0.3, 0.1, 0.3, 0.55, 0.35, 0.35, 0.25, 0.45)^T$.

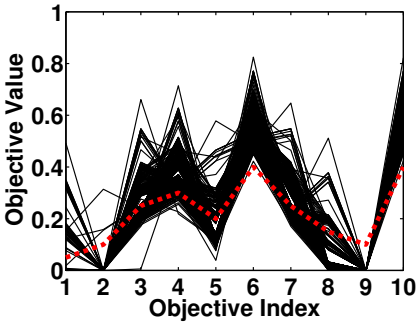

(a) MOEA/D-STM

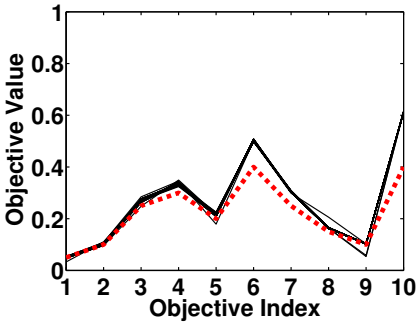

(b) R-NSGA-II

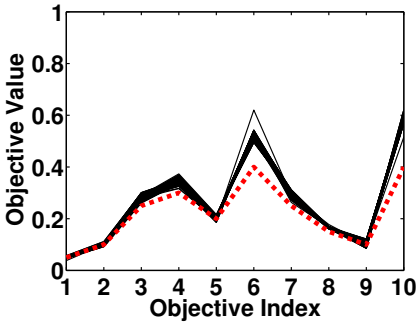

(c) r-NSGA-II

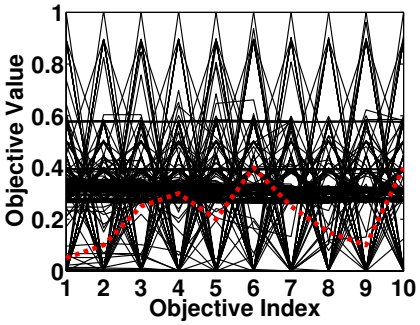

(d) NSGA-III

Figure 32: Comparisons on 10-objective DTLZ4 where $\mathbf{z}^r = (0.05, 0.1, 0.25, 0.3, 0.2, 0.4, 0.25, 0.15, 0.1, 0.4)^T$.

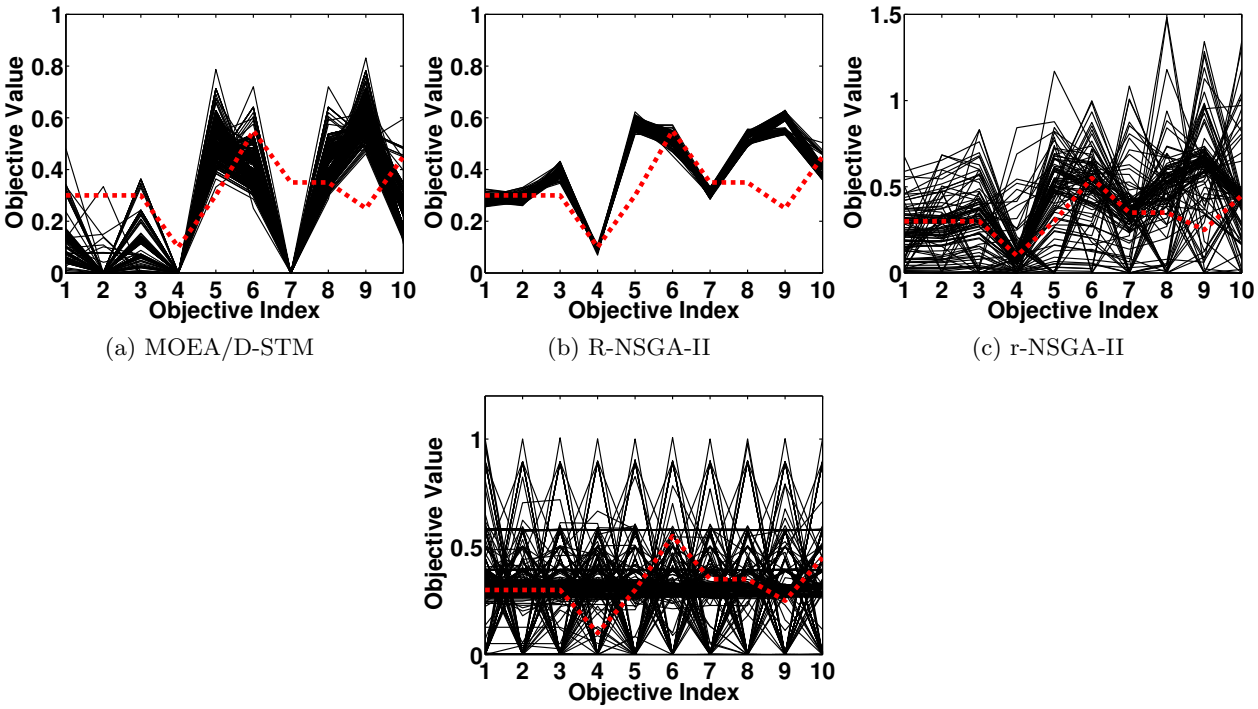

(a) MOEA/D-STM (b) R-NSGA-II (c) r-NSGA-II

(d) NSGA-III

Figure 33: Comparisons on 10-objective DTLZ4 where $\mathbf{z}^r = (0.3, 0.3, 0.3, 0.1, 0.3, 0.55, 0.35, 0.35, 0.25, 0.45)^T$.